Repositório ISCTE-IUL

Impact of Traffic Load and Spectral Occupancy on Gaussian Noise Models Performance for Multiband Networks

Pedro Venda[*], João Rebola[*†], Luís Cancela[*†]

[*]Instituto Universitário de Lisboa (ISCTE-IUL), Lisboa, Portugal

[†]Optical Communications and Photonics Group, Instituto de Telecomunicações, Lisboa, Portugal

E-mail: pdsva@iscte-iul.pt, joao.rebola@iscte-iul.pt, luis.cancela@iscte-iul.pt

Abstract—In a network scenario, wavelength division-multiplexing channels are added and dropped leading to fluctuations on the network traffic loads along the optical path. In this work, a comparison between the optical signal-to-noise ratio (OSNR) predictions of the recently proposed closed-form generalized Gaussian noise (GGN) model and a closed-form Gaussian noise (GN) model that does not take into account the stimulated Raman scattering (SRS) is performed, for different network traffic loads and spectral occupancy over the entire C+L band. In all results obtained, the maximum difference between the OSNR predictions of GN (without SRS) and GGN models closed forms is below 0.7 dB at optimum OSNR and maximum C+L band occupancy, indicating that the GN-model can also be used in C+L band transmission. For channel launch powers higher than the optimum, the OSNR differences increase up to 3 dB, being the GN-model (without SRS) unsuitable to assess the network performance in such situations.

I. Introduction

The Gaussian-noise (GN) model is an efficient and widely adopted tool to estimate the nonlinear interference (NLI) due to Kerr nonlinearity, simplifying current wavelength-division multiplexing (WDM) systems design and analysis [1], [2]. Recently, the generalized Gaussian-noise (GGN) model has been proposed for assessing the performance of multiband C+L transmission in WDM optical systems, where the interaction between NLI and stimulated Raman scattering (SRS) must be accurately characterized [3]–[5].

For C-band transmission, various closed-form GN-model approximations have been proposed over the years [1], [6]–[9], while, recently, GGN-model closed formulas have been derived for transmission networks operating beyond the C-band [5], [10], the so-called multiband networks. For optical networking, both GN and GGN models closed forms allow fast and reliable analysis of the network physical layer impairments, enabling the development and implementation of more rigorous real time network optimization tools [1], [5], [11].

In reconfigurable optical add/drop multiplexer (ROADM) based networks, the WDM channels can be added, dropped or expressed [12], leading to dynamic traffic variations in the fiber spans. Thus, the number and the power of WDM channels transmitted in a given span of a given lightpath vary constantly, meaning that the WDM signal bandwidth does not always fully covers the span maximum capacity, and consequently, the full network capacity. Network performance studies using the GGN-model have been presented in [13], [14]. In [13], the capacity gain of reducing the link margin is studied in a dynamic scenario considering the C+L band and a blocking probability of 10%, which can be considered too high for network normal operation [15], [16]. In [14], a comparison between a worst-case network with a full C+L band occupancy and the same unlikely dynamic traffic case with the 10% blocking probability is performed. In [5], a preliminary study of the effect of the dynamic traffic variations on NLI predictions using a closed-form GGN-model was carried out for validation purposes, without assessing its impact on the optical signal-to-noise ratio (OSNR).

In this work, the closed-form GGN-model introduced in [5] is investigated against the closed-form GN-model [9] proposed for C-band network transmission and their accuracy for performance estimation in C+L mulitband systems is discussed, which to the best of our knowledge has not been done yet. The accuracy of the OSNR predictions is assessed using both models, considering fluctuations on the traffic loads along the lightpath of the network, increasingly filling the WDM spectral occupancy up to the full range of C+L band and taking into account the effect of the add/drop operations on the OSNR.

This paper is organized as follows. In section II, the main definitions and assumptions of the optical network simulator developed to account for dynamic traffic load and variable WDM channels spectral occupation are presented and explained. In section III, the performance of the two closed-form GN models is compared and the impact of the network traffic load, channels add/drop and spectral occupancy on the OSNR estimation is quantified. Section IV presents the conclusions.

II. Network Simulation

In this section, the simulator developed for assessing the performance of a multiband optical network and related assumptions are presented and explained.

The two lightpaths examples studied in this work, taken from the British Telecommunications network topology [5], are illustrated in Fig. 1. The ROADMs architecture considered for the optical node is the route-and-select with maximum losses of 18 dB [17]. The filtering effects and crosstalk due to ROADM components imperfections [18] are not taken

(a)

(b)
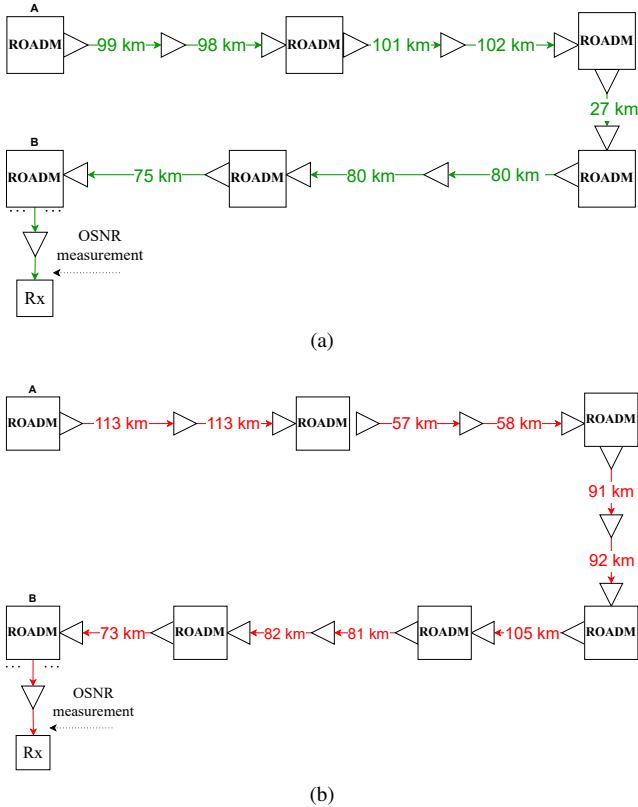
Fig. 1. Two lightpaths examples taken from the British Telecommunications topology of the United Kingdom core network [5]. Throughout this work, the lightpaths in (a) and (b) are referred to as green and red lightpaths, respectively.

into account in this work. The post-amplifiers are designed to perfectly compensate the ROADM losses. The inline and pre-amplifiers compensate perfectly the previous fiber losses. All optical amplifiers considered in the lightpaths are erbium doped fiber amplifiers (EDFAs) with dynamic gain equalization [3]. Thus, the EDFAs also compensate the power transfer in each span due to SRS.

For the analysis of the lightpaths represented in Fig. 1, the WDM channels are classified in two categories: channels under test (CUTs) and add/drop channels. The CUTs correspond to the WDM channels that are transmitted along the complete lightpath, i.e., from the first node to the last node without any add/drop occurring in those wavelengths. The add/drop channels are the wavelengths that can be added or dropped in any ROADM of the considered lightpath. We also introduce the two following definitions: *network utilization* and *C+L band occupancy*. For a given span of a lightpath, the ratio between the number of channels transmitted in the j-th span and the total number of channels is defined as span utilization, which is denoted as $\epsilon_{\mathrm{span},j}$. For the entire lightpath, the network utilization $\epsilon_{\mathrm{network}}$ is defined as the average of the network utilizations of all spans, written as

$$\epsilon_{\mathrm{network}} = \frac{1}{N_s} \sum_{j=1}^{N_s} \epsilon_{\mathrm{span},j} = \frac{1}{N_s} \sum_{j=1}^{N_s} \frac{N_{ch,j}}{N_{ch}} \quad (1)$$

where $N_{ch,j}$ is the number of channels transmitted in the j-th span, N_s is the number of spans in the lightpath and N_{ch} is the total number of WDM channels considered. The C+L band occupancy $\epsilon_{\mathrm{occupancy}}$ is defined as

$$\epsilon_{\mathrm{occupancy}} = \frac{\Delta f N_{ch}}{B_{\mathrm{C+L\text{-}band}}} \quad (2)$$

where Δf is the channel spacing and $B_{\mathrm{C+L\text{-}band}}$ is the total C+L optical transmission bandwidth, assumed as 11.5 THz [19], which corresponds to 100% C+L band occupancy.

In order to emulate the behavior of dynamic traffic load variations occurring in each ROADM node, we consider that the add/drop channels are added or dropped randomly following a uniform distribution. The number of add/drop channels depends on the required $\epsilon_{\mathrm{network}}$. The launch power of the added channels has a random offset of $\pm 1\,\mathrm{dB}$ relative to the launch power of the CUTs and, for a more realistic approach, the added channels always maintain the same power until they are dropped, i.e., for a given lightpath, the power of a channel only changes if it is added to the optical network more than one time. This last assumption differs from the optical transmission scenario considered in [5], where the add/drop channels that have not been dropped may not maintain the power they had in the previous span. The launch powers of the CUTs remain the same along the complete lightpath.
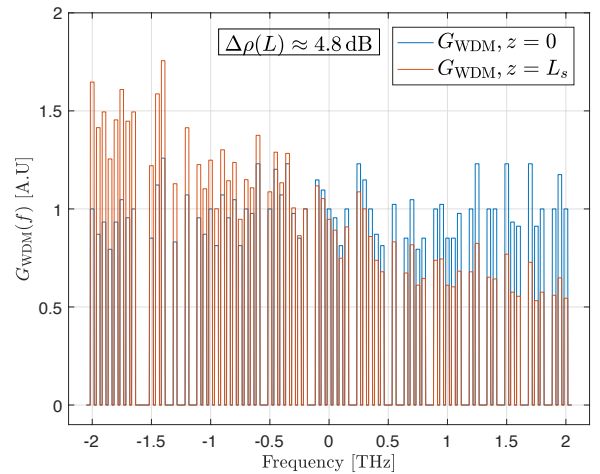
Fig. 2. Randomly generated normalized PSD of a WDM signal transmitted in a network scenario, at the input ($z = 0$) and at the end ($z = L_s$) of a span, for $\epsilon_{\mathrm{network}} = 80\%$ and $\epsilon_{\mathrm{occupancy}} \approx 35\%$. Blue lines: WDM signal PSD at $z = 0$. Orange lines: WDM signal PSD at $z = L_s$.

A randomly generated normalized power spectral density (PSD) of a transmitted WDM signal $G_{\mathrm{WDM}}(f)$ is shown in Fig. 2, at the input $z = 0$ and at the end $z = L_s$ of a fiber span, for a network utilization $\epsilon_{\mathrm{network}} = 80\%$ and a C+L band occupancy $\epsilon_{\mathrm{occupancy}} \approx 35\%$. The WDM signal PSDs shown are normalized to the PSD value of the CUTs. Notice that, as a consequence of the considered scenario with $\epsilon_{\mathrm{network}} = 80\%$, there is the presence of unused channel frequency slots and oscillations in the PSD amplitudes. For

$z = 0$, these oscillations are only a consequence of the add/drop channels having a launch power with a random offset of $\pm 1\,\mathrm{dB}$ relative to CUTs power. For $z = L_s$, i.e., after the WDM signal has been transmitted through the optical fiber, the PSD variation is tilted due to the impact of the SRS, which causes a power transfer $\Delta\rho(L) \approx 4.8\,\mathrm{dB}$ from higher to lower frequency components.

All NLI contributions along an optical link composed by several fiber spans sum coherently or incoherently along the signal propagation until the receiver [6]. The coherent and incoherent variants of the GGN-model will be studied and referred as the coherent GGN-model and incoherent GGN-model, respectively. Due to the asymptotic expansion of the dilog function performed in its derivation, we will refer to the GN-model proposed for the C-band as the asymptotic GN-model [9]. It is important to notice that this model considers that the NLI accumulates incoherently along the optical path. It should be noted that among the GN models studied, the coherent GGN-model is the one that provides more accurate estimates of the normalized NLI power η_{NLI} in comparison with the split-step Fourier method [5], and therefore, it is the more accurate model to estimate the OSNR. The network simulator used in this work has been successfully validated by obtaining the results shown in Fig. 8 of [5].

III. GN MODELS COMPARISON

In the following, the impact of the network utilization and C+L band occupancy on the OSNR estimation using the GGN-model [5, Eq. (5)] and the asymptotic GN-model [9, Eq. (16)] is evaluated. The system parameters considered for the OSNR calculation are presented in Table I. In this work, we assume that the impact of the SRS on the ASE noise power is negligible.

In order to assess the optimum optical power, in Fig. 3, the OSNR is shown as a function of the SRS power transfer between the WDM outer channels $\Delta\rho(L)$, for $\epsilon_{\mathrm{occupancy}} = 87\%$, $\epsilon_{\mathrm{network}} = 90\%$ and for the channels at the following frequencies: -5, -2.5, 0, 2.5 and 5 THz. The power transfer is increased by increasing the CUTs launch power [3].

For the center channel, the CUTs launch power of approximately 0 dBm leads to the power transfer of around 4 dB that allows obtaining the maximum OSNR, for both lightpaths. For this optimum power, i.e., when the OSNR maximum is reached in Fig. 3, the maximum OSNR variation between the five WDM channels is only about 0.7 dB.

A. OSNR over the C+L band at optimum launch power

The OSNR and power transfer $\Delta\rho(L)$ as a function of the C+L band occupancy are shown in Fig. 4(a) for the WDM lowest frequency channel, in Fig. 4(b) for the center channel and in Fig. 4(c) for the highest frequency channel. The network utilization considered is about 95% and the CUTs power is set to $P_{CUT} = 0\,\mathrm{dBm}$, which, for the C+L band system studied, leads approximately to the maximum OSNR for all WDM channels, as shown in Fig. 3. The lowest, center and highest frequency channels are always assumed to be CUTs. Using an
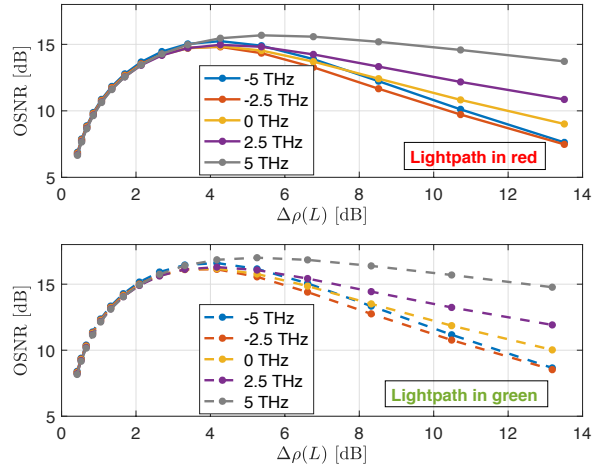
Fig. 3. OSNR as a function of the power transfer between the outer channels $\Delta\rho(L)$, for $\epsilon_{\mathrm{occupancy}} = 87\%$, $\epsilon_{\mathrm{network}} = 90\%$, $N_{CUT} = 20\% \cdot N_{ch}$ and the red and green lightpaths.

TABLE I
SYSTEM PARAMETERS FOR SECTION III

System parameters	
Maximum number of WDM of channels (N_{ch})	201
Number of channels under test (N_{CUT})	41
Symbol rate (R_s) [GBaud]	32
Channel bandwidth (B_m) [GHz]	32
Loss coefficient (α) [dB/km]	0.22
Dispersion (β_2) [ps/nm/km]	16.7
Dispersion slope (S_r) [ps/nm^2/km]	0.067
NLI coefficient (γ) [W^{-1}.km^{-1}]	1.3
Raman gain slope (C_r) [W^{-1}km^{-1}THz^{-1}]	0.028
EDFA noise figure (F_n) [dB]	5

uniform distribution, the remaining CUTs are chosen randomly until 20% of the available WDM channels are occupied, i.e., $N_{CUT} = 20\% N_{ch}$. Two channels spacings are considered: 50 GHz (blue lines) and 100 GHz (yellow lines). To increase the C+L band occupancy, the channels are added sequentially in the total available bandwidth, i.e., first, the C-band is filled and then the L-band. The division that marks the end of the C-band and the beginning of the L-band is highlighted by dashed black vertical lines.

In Fig. 4(b), for the center channel and the two channel spacings, the OSNR predictions using the asymptotic GN-model show a very good agreement with the ones obtained with the incoherent GGN-model for all the values of the C+L band occupancy. Due to higher NLI predictions, the coherent GGN-model provides lower OSNRs in the center channel, with a 0.2 dB maximum difference relative to the other two GN models. When comparing to the incoherent GGN-model results, it can be seen that, for $\Delta f = 50\,\mathrm{GHz}$ and a $\epsilon_{\mathrm{occupancy}}$ above 70%, the asymptotic GN-model overestimates and underestimates the OSNR for the lowest and highest WDM frequencies,
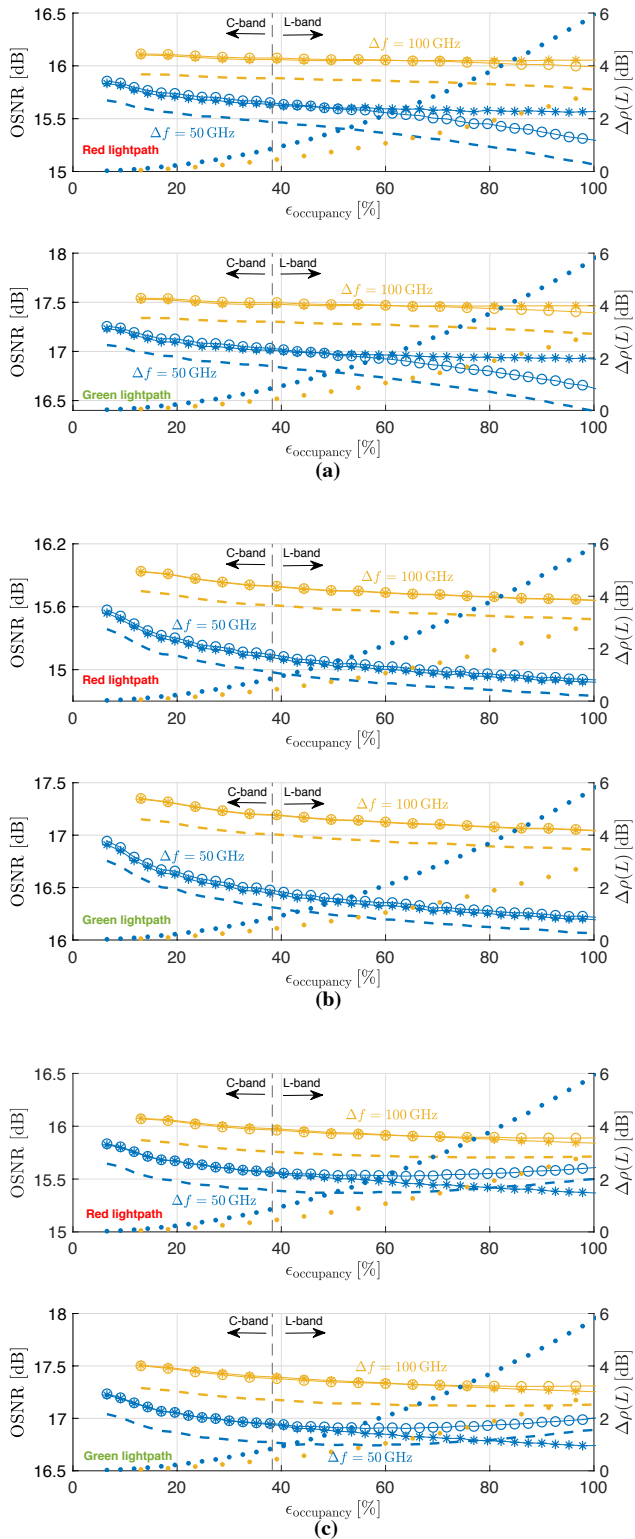
Fig. 4. OSNR for the red and green lightpaths as a function of the C+L band occupancy, for the center channel in (b) and the lowest and highest WDM frequency channels in (a) and (c), respectively. The network utilization is 95% and $N_{CUT} = 20\% \cdot N_{ch}$. Circles: closed form GGN-model (incoherent). Dashed lines: closed form GGN-model (coherent). Asterisks: asymptotic GN-model. Points: $\Delta\rho(L)$.

respectively. When the C+L band is completely filled and the average power transfer is approximately 6 dB, the difference in OSNR between these models reaches its maximum with 0.3 dB. The maximum OSNR discrepancy between the asymptotic GN-model and the coherent GGN-model is about 0.5 dB and is reached for $\Delta f = 50\,\text{GHz}$ and $\epsilon_{\text{occupancy}} = 100\%$. These higher OSNR discrepancies encountered for $\Delta f = 50\,\text{GHz}$ are due to the higher SRS power transfer relative to the one obtained for the 100 GHz channel spacing. The OSNR differences between the GN models are approximately the same for both lightpaths considered.

B. OSNR considering different CUTs launch powers

In Fig. 5, the OSNR for only the red lightpath is depicted as a function of the CUTs frequencies, for (a) $P_{CUT} = -3\,\text{dBm}$, (b) $P_{CUT} = 0\,\text{dBm}$ and (c) $P_{CUT} = 3\,\text{dBm}$, for $\epsilon_{\text{occupancy}} = 100\%$ and $\epsilon_{\text{network}} = 95\%$. In contrast to the closed-form GGN-model, the asymptotic GN-model does not take into account the influence of the dispersion slope on the NLI prediction. For a fair comparison, in these results, a null dispersion slope is considered in the OSNR estimation by the GGN models. The remaining system parameters are presented in Table I.

In Fig. 5(a), since there is no considerable SRS power transfer for launch powers below 0 dBm, the difference between the OSNRs is below 0.3 dB for all the GN-models considered. In Fig. 5(b), it can be seen that, due to the enhancement of the SRS effect caused by increasing the optical launch power to 0 dBm, the maximum discrepancy between the asymptotic GN-model and incoherent and coherent GGN models increases to about 0.4 dB and 0.7 dB, respectively. In Fig. 5(c), the considered CUTs power surpasses the optimal power of 0 dBm, and due to SRS, a much sharper tilt in the OSNR can be observed in the GGN-model results. The maximum average power transfer rises, respectively, from 6 dB to 11.9 dB, for the 50 GHz channel spacing, and from 3 dB to 5.9 dB for the 100 GHz spacing, in relation to the 0 dBm launch power. Consequently, the maximum OSNR difference between the asymptotic estimation and coherent and incoherent GGN models increases, respectively, to about 3 dB and 2.4 dB. Notice that the OSNR variation along the CUTs frequency given by the asymptotic GN-model does not predict the OSNR tilt, leading to higher OSNR discrepancies for more pronounced OSNR tilts.

As a main conclusion, the results presented in this subsection show that the asymptotic GN-model can provide reasonably accurate OSNR predictions in C+L band optical networks at optimum launch power, but can lead to differences in the OSNR of up to 3 dB, when the launch power leads to a significant SRS effect.

C. OSNR for different network utilizations

Lastly, it is important to analyze how the network utilization impacts the performance of the GN models when the WDM signal covers the full C+L band, i.e., $\epsilon_{\text{occupancy}} = 100\%$. The OSNR as a function of $\epsilon_{\text{network}}$ is represented in Fig. 6(a) for
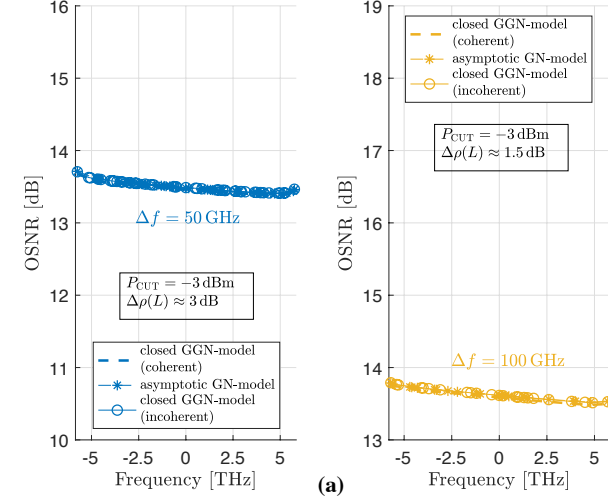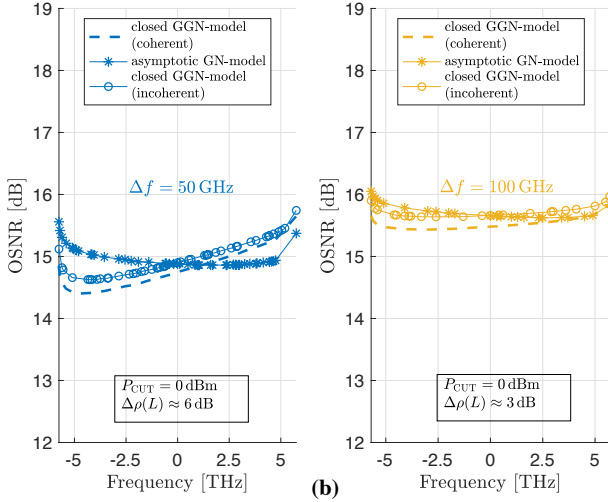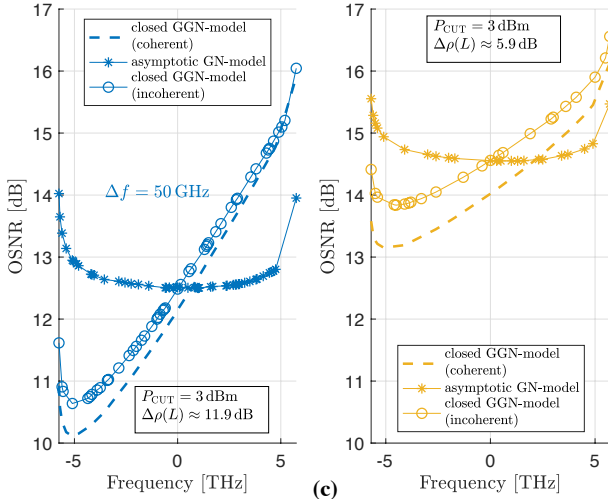
Fig. 5. OSNR for the red lightpath as a function of the CUTs frequencies, for $\epsilon_{\text{occupancy}} = 100\%$, $\epsilon_{\text{network}} = 95\%$, $N_{CUT} = 20\% \cdot N_{ch}$, $S_r = 0$ and the launch powers of (a) -3 dBm, (b) 0 dBm and (c) 3 dBm. Channel spacings $\Delta f = 50\,\text{GHz}$ and $\Delta f = 100\,\text{GHz}$ are considered. Circles: closed-form GGN-model (incoherent). Dashed lines: closed-form GGN-model (coherent). Asterisks: asymptotic GN-model. Points: $\Delta\rho(L)$.
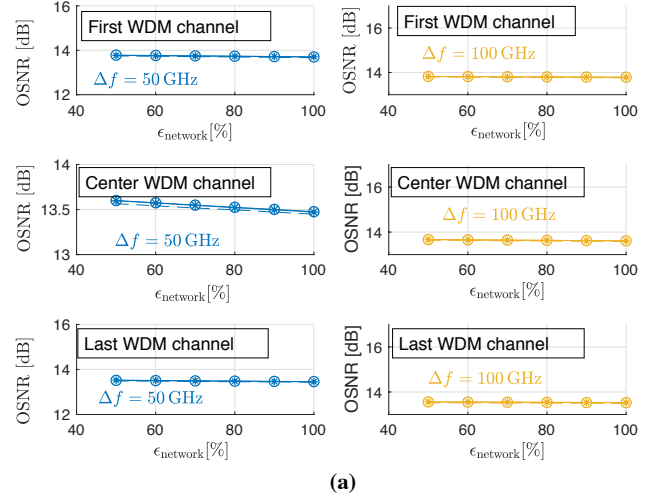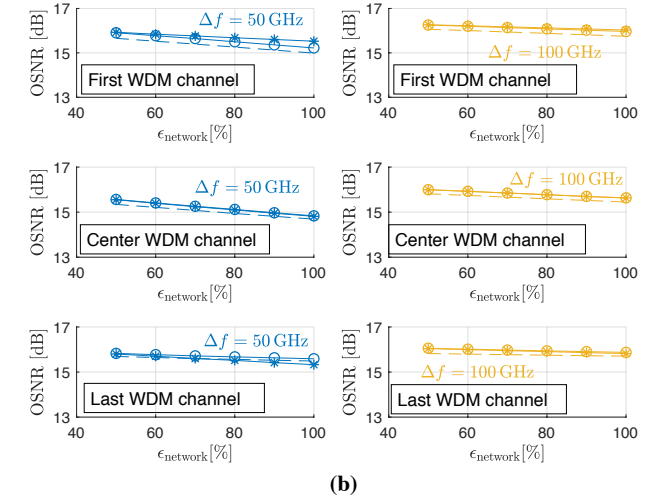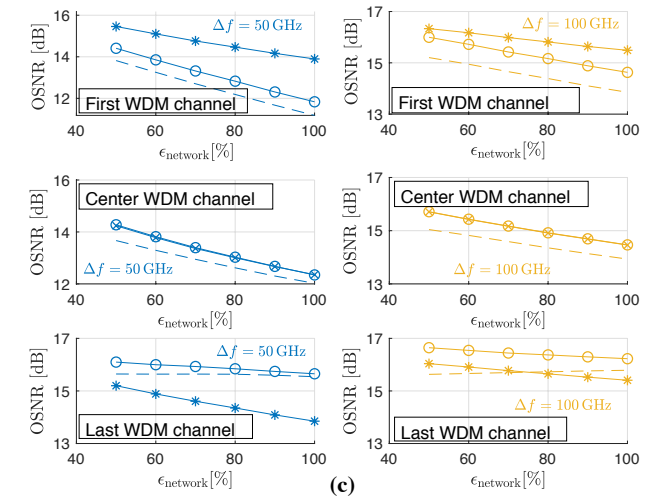
Fig. 6. OSNR for the red lightpath as a function of the network utilization, for (a) $P_{CUT} = -3\,\text{dBm}$, (b) $P_{CUT} = 0\,\text{dBm}$ and (c) $P_{CUT} = 3\,\text{dBm}$. Only results for the first (-5.7 THz), center and last (5.7 THz) WDM channels are presented. The channel spacings $\Delta f = 50\,\text{GHz}$ and $100\,\text{GHz}$ are used. Lines with circles: closed-form GGN-model (incoherent). Dashed lines: closed-form GGN-model (coherent). Lines with asterisks: asymptotic GN-model.

$P_{\text{CUT}} = -3\,\text{dBm}$, in Fig. 6(b) for $P_{\text{CUT}} = 0\,\text{dBm}$ and in Fig. 6(c) for $P_{\text{CUT}} = 3\,\text{dBm}$. For convenience, it is assumed that the lowest and highest frequency channels correspond to the first and last channels of the WDM signal, respectively.

The good agreement between the models predictions for $P_{\text{CUT}} = -3\,\text{dBm}$ is due to the lower power transfer of only 3.1 dB, which occurs when $\epsilon_{\text{network}} = 100\%$ and $\Delta f = 50\,\text{GHz}$. For $P_{\text{CUT}} = 0\,\text{dBm}$, the overall power transfer increases, leading to higher differences between the OSNR estimates as the network utilization increases, as can be observed in Fig. 6 (b). The OSNR differences using the incoherent GGN-model and the asymptotic GN-model reach 0.3 dB in the edge channels, when $\epsilon_{\text{network}} = 100\%$ and $\Delta \rho(L) \approx 6.2\,\text{dB}$. For the coherent GGN-model and for $\Delta f = 50\,\text{GHz}$, the OSNR differences in the first channel relative to the asymptotic GN-model are about 0.3 dB and 0.5 dB for $\epsilon_{\text{network}} = 50\%$ and $\epsilon_{\text{network}} = 100\%$, respectively. For $\Delta f = 100\,\text{GHz}$, this discrepancy is always below about 0.3 dB. For the last channel, the OSNR estimates are very similar to the estimates of the asymptotic GN-model for all $\epsilon_{\text{network}}$ considered. For $P_{\text{CUT}} = 3\,\text{dBm}$, the OSNR predictions from the GN models follow a similar behavior as with $P_{\text{CUT}} = 0\,\text{dBm}$, but due to the higher power transfer, the OSNR prediction deviations between the models for the edge channels become larger, for all network utilizations considered. For instance, for the first channel with $\Delta f = 50\,\text{GHz}$, the asymptotic GN-model overestimates the OSNR at least by about 1 dB and 2 dB for $\epsilon_{\text{network}} = 50\%$ and $\epsilon_{\text{network}} = 100\%$, respectively. For $\Delta f = 100\,\text{GHz}$, a maximum OSNR difference of about 1.6 dB occurs for the first WDM channel and $\epsilon_{\text{network}} = 100\%$.

IV. CONCLUSION

In this work, we studied the impact of the network utilization and C+L band occupancy on the OSNR estimation using closed-form GN models. Comparing the performances of the asymptotic and GGN models in optimum OSNR conditions and for the full C+L band occupancy, the maximum OSNR difference using the asymptotic GN-model is only 0.7 dB compared to the optimum OSNR obtained with the GGN-model. Hence, we have shown that, at optimum launch power and for applications that do not have high accuracy requirements, the asymptotic GN-model can represent a viable alternative to estimate the NLI in C+L band transmissions systems for power transfers below 6 dB. Furthermore, is is expected that most optical networks are working near this low nonlinear effects regime [3]. However, for higher launch powers that lead to higher SRS power transfer, the OSNR discrepancies can increase up to 3 dB. Therefore, the use of the asymptotic GN-model is not recommended in this case. Moreover, in this work, we also showed that higher network utilizations lead to an increasing impact of the SRS, which increases the NLI impact and decreases the overall network performance.

ACKNOWLEDGMENT

REFERENCES

[1] P. Poggiolini and Y. Jiang, "Recent advances in the modeling of the impact of nonlinear fiber propagation effects on uncompensated coherent transmission systems," *J. Lightw. Technol.*, vol. 35, no. 3, pp. 458–480, Feb. 2017.

[2] A. Ferrari *et al.*, "GNPy: an open source application for physical layer aware open optical networks," *J. Opt. Commun. Netw.*, vol. 12, no. 6, pp. C31–C40, Jun. 2020.

[3] D. Semrau, R. I. Killey, and P. Bayvel, "The Gaussian noise model in the presence of inter-channel stimulated Raman scattering," *J. Lightw. Technol.*, vol. 36, no. 14, pp. 3046–3055, Jul. 2018. arXiv: 1801.02460.

[4] M. Cantono, J. L. Auge, and V. Curri, "Modelling the impact of SRS on NLI generation in commercial equipment: an experimental investigation," in *Proc. Opt. Fiber Commun. Conf. Expo.*, San Diego, CA, USA, Mar. 2018, paper M1D.2.

[5] D. Semrau, R. I. Killey, and P. Bayvel, "A closed-form approximation of the gaussian noise model in the presence of inter-channel stimulated raman scattering," *J. Lightw. Technol.*, vol. 37, no. 9, pp. 1924–1936, May 2019.

[6] P. Poggiolini, "The GN model of non-linear propagation in uncompensated coherent optical systems," *J. Lightw. Technol.*, vol. 30, no. 24, pp. 3857–3879, Dec. 2012.

[7] X. Chen and W. Shieh, "Closed-form expressions for nonlinear transmission performance of densely spaced coherent optical OFDM systems," *Opt. Express*, vol. 18, no. 18, pp. 19 039–19 054, Aug. 2010.

[8] S. J. Savory, "Approximations for the nonlinear self-channel interference of channels with rectangular spectra," *IEEE Photon. Technol. Lett.*, vol. 25, no. 10, pp. 961–964, May 2013.

[9] P. Johannisson and E. Agrell, "Modeling of nonlinear signal distortion in fiber-optic networks," *J. Lightw. Technol.*, vol. 32, no. 23, pp. 4544–4552, Dec. 2014.

[10] D. Semrau, R. Killey, and P. Bayvel, "Achievable rate degradation of ultra-wideband coherent fiber communication systems due to stimulated raman scattering," *Opt. Express*, vol. 25, no. 12, pp. 13 024–13 034, Jun. 2017.

[11] V. Anagnostopoulos, C. T. Politi, C. Matrakidis, and A. Stavdas, "Physical layer impairment aware wavelength routing algorithms based on analytically calculated constraints," *Opt. Commun.*, vol. 270, no. 2, pp. 247–254, Feb. 2007.

[12] S. Gringeri, B. Basch, V. Shukla, R. Egorov, and T. J. Xia, "Flexible architectures for optical transport nodes and networks," *IEEE Commun. Mag.*, vol. 48, no. 7, pp. 40–50, Jul. 2010.

[13] A. Mitra *et al.*, "Effect of reduced link margins on C+L band elastic optical networks," *J. Opt. Commun. Netw.*, vol. 11, no. 10, pp. C86–C93, Oct. 2019.

[14] A. Mitra *et al.*, "Effect of channel launch power on fill margin in C+L band elastic optical networks," *J. Lightw. Technol.*, vol. 38, no. 5, pp. 1032–1040, Mar. 2020.

[15] N. Sambo *et al.*, "Provisioning in multi-band optical networks," *J. Lightw. Technol.*, vol. 38, no. 9, pp. 2598–2605, May 2020.

[16] B. Correia, R. Sadeghi, E. Virgillito, A. Napoli, N. Costa, J. Pedro, and V. Curri, "Power control strategies and network performance assessment for C+ L+ S multiband optical transport," *J. Opt. Commun. Netw.*, vol. 13, no. 7, pp. 147–157, Jul. 2021.

[17] J. Pedro, "Designing transparent flexible-grid optical networks for maximum spectral efficiency [invited]," *IEEE/OSA J. Opt. Commun. Netw.*, vol. 9, no. 4, pp. C35–C44, Apr. 2017.

[18] D. Sequeira, L. Cancela, and J. Rebola, "CDC ROADM design tradeoffs due to physical layer impairments in optical networks," *Opt. Fiber Technol.*, vol. 62, p. 102 461, Mar. 2021.

[19] A. Ferrari *et al.*, "Assessment on the achievable throughput of multi-band ITU-T G.652.D fiber transmission systems," *J. Lightw. Technol.*, vol. 38, no. 16, pp. 4279–4291, Aug. 2020.